Numerical analysis of the immersed boundary method applied to the flow around a forced oscillating cylinder

FLUIDOS 2010: XI Meeting on Recent Advances in the Physics of Fluids and their Applications IOP Publishing
Journal of Physics: Conference Series **296** (2011) 012011 doi:10.1088/1742-6596/296/1/012011

Numerical analysis of the immersed boundary method applied to the flow around a forced oscillating cylinder

L. C. Pinto[1], E. B. C. Schettini[2] and J. H. Silvestrini[3]

[1,2]Instituto de Pesquisas Hidráulicas, Universidade Federal do Rio Grande do Sul, Av. Bento Gonalves 9500, 91501-970, Porto Alegre - RS - Brazil
[3]Faculdade de Engenharia, Pontifícia Universidade Católica do Rio Grande do Sul, Av. Ipiranga 6681, 90619-900, Porto Alegre - RS - Brazil

E-mail: [1]leandroconp@gmail.com,[2]bcamano@iph.ufrgs.br,[3]jorgehs@pucrs.br

Abstract. In present paper, Navier-Stokes and Continuity equations for incompressible flow around an oscillating cylinder were numerically solved. Sixth order compact difference schemes were used to solve the spatial derivatives, while the time advance was carried out through second order Adams Bashforth accurate scheme. In order to represent the obstacle in the flow, the Immersed Boundary Method was adopted. In this method a force term is added to the Navier-Stokes equations representing the body. The simulations present results regarding the hydrodynamic coefficients and vortex wakes in agreement to experimental and numerical previous works and the physical lock-in phenomenon was identified. Comparing different methods to impose the IBM, it can be concluded that no alterations regarding the vortex shedding mode were observed. The Immersed Boundary Method techniques used here can represent the surface of an oscillating cylinder in the flow.

1. Introduction

The applications of the study of flow around oscillating bodies are diverse. The process of oil extraction from deep waters, for example, can be done through floating platforms, which are equipped with slender, cylindrical structures, called risers. Risers are responsible to conduct the oil from the bottom of the sea to the platform. Another important application is concerned to the study of the oscillating macrophyte vegetation in lakes and watercourses. Emerging macrophytes prominently in lakes can start a movement caused by external agents, as wind or waves, changing its morphology.

When a cylinder is oscillating, significant changes can be observed in the flow. Studies by [1] showed that, if the oscillation has well-defined frequency and amplitude displacement, the vortex street wakes presents characteristics shedding modes. Those authors mapped such modes, and introduced a symbolic code classification of letters and numbers, describing the combination of paired or simple vortex shedding during each forced oscillation cycle of the cylinder.

According the experiments by [2], when the oscillation frequency (f_o) is close to the frequency corresponding to the Strouhal number (f_s), a certain control in the vortex shedding is caused by the cylinder oscillation. It could be observed only for a range of f_o and up to a certain oscillation amplitude. This phenomenon is usually known as *lock-in*.

In this paper, results of hydrodynamic coefficients and instantaneous vorticity fields were compared to identify which numerical technique best represents the solid boundaries of the oscillating cylinder in the flow.

2. Numerical Methodology

The incompressible Navier-Stokes and the continuity equations:

$$\frac{\partial \mathbf{u}}{\partial t} = -\boldsymbol{\nabla} p - \frac{1}{2}[\boldsymbol{\nabla}(\mathbf{u} \otimes \mathbf{u}) + (\mathbf{u} \cdot \boldsymbol{\nabla})\mathbf{u}] + \frac{1}{Re}\boldsymbol{\nabla}^2 \mathbf{u} + \mathbf{f}, \tag{1}$$

$$\boldsymbol{\nabla} \cdot \mathbf{u} = 0, \tag{2}$$

are directly solved on a computational grid in non-staggered configuration. In this equations, $\mathbf{u}$ and p are the velocity and pressure fields, respectively, and Re is the non-dimensional Reynolds Number. The present computational code, called `Incompact3d`, uses sixth order compact difference schemes to solve the spatial derivatives, while the time advance was carried out through second order Adams-Bashforth accurate scheme. In order to represent the obstacle in the flow we used here an Immersed Boundary Method (IBM), which is based on the addition of a forcing term in the flow governing equations to model the presence of the body. The direct forcing term $\mathbf{f}$ can be expressed as:

$$\mathbf{f} = \varepsilon\{\frac{1}{2}[\boldsymbol{\nabla}(\mathbf{u} \otimes \mathbf{u}) + (\mathbf{u} \cdot \boldsymbol{\nabla})\mathbf{u}] - \frac{1}{Re}\boldsymbol{\nabla}^2 \mathbf{u} + \boldsymbol{\nabla} p + \frac{\mathbf{u}_o - \mathbf{u}}{\Delta t})\}, \tag{3}$$

with $\varepsilon = 1$ in the body, and 0 everywhere else. The no-slip condition in the moving boundaries is obtained when:

$$\mathbf{u}(D/2, \theta, z, t) = \mathbf{u}_d, \tag{4}$$

where $\mathbf{u}_d$ is the forced oscillating cylinder velocity. The target velocity $\mathbf{u}_o$ is calibrated by the external velocity field and an artificial flow is created inside the cylinder. According to [3], a formal expression to $\mathbf{u}_o$ can be given as:

$$\mathbf{u}_o(r, \theta, z, t) = \mathbf{u}_d + [\mathbf{u}_d - \mathbf{u}(D - r, \theta, z, t)]g(r), \tag{5}$$

with

$$g(r) = sin(\frac{2\pi r^2}{D^2}). \tag{6}$$

The principle of direct forcing is to preserve the no-slip boundary condition avoiding discontinuities in the first derivative at the cylinder surface [4].

The oscillating cylinder velocity $\mathbf{u_d}$ is defined from the cylinder displacement, which can be expressed by $y_c = y_0 + A/Dcos(2\pi f_o t)$, where y_0 is the initial coordinate cylinder and A/D the non-dimensional displacement amplitude based on the diameter of the cylinder (D).

The equations (1) and (2) are solved in a computational domain $L_x \times L_y$ discretized on a Cartesian mesh of $n_x \times n_y$ nodes. Free-slip boundary conditions are assumed at the lateral boundaries ($y = 0$, $y = L_y$) while in the streamwise direction (inflow/outflow boundary) are imposed as velocity Dirichlet conditions. At the inlet ($x = 0$), an streamwise uniform profile (U) is prescribed while at the outlet ($x = L_x$), an one-dimensional convection equation is solved.

Regarding the validation, studies as [4, 5, 6, 7] using `Incompact3d`, presented both qualitatively and quantitatively results for conventional and complex flow geometries around fixed obstacles. According such studies, the code is a very attractive tool for solving flows in the context of Direct Numerical Simulations (DNS). Here, it was used in two-dimensional configuration.

3. Results

Simulations for oscillating cylinder with the frequency ratio $F = f_o/f_s$ varied from 0.8 to 1.2 were performed using the computational grid n_x, n_y = 361, 217 (and 325) and the computational domain L_x, L_y = $20D$, $12D$ (and $18D$). In all simulations, the parameters Re = 185 and $A/D = 0.2$ were constants. A fixed time step $\Delta t = 0.005D/U$ is used in order to ensure both convective (Courant-Friedrich-Levy) and diffusive criteria.

3.1. Hydrodynamic coefficients

The results of the mean drag $<C_D>$ and root mean square lift C_{Lrms} coefficients varying the frequency ratio $F = f_o/f_s$ are compared in figure 1 with other authors [8, 9].

The numerical simulations by [8] were done with the computational grid n_x,n_y = 1201, 1201 and the computational domain L_x, L_y = $24D$, $24D$. The IBM was implemented using the feedback forcing technique based on an artificial term that can "freezes" the fluid in the body region through a damping oscillation process.

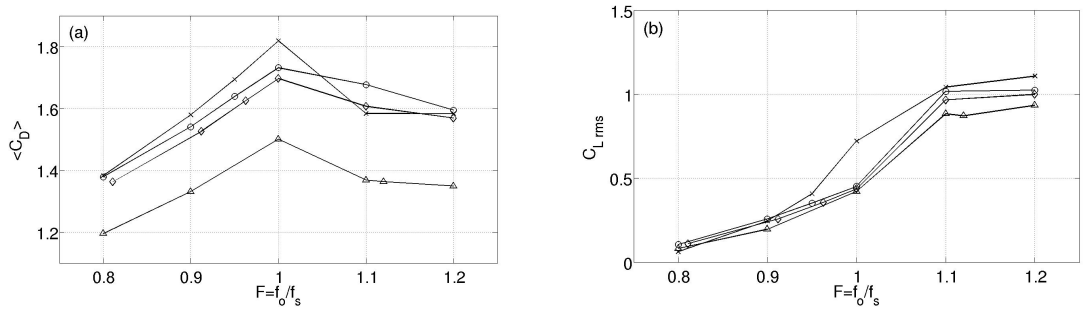

Figure 1. Force coefficients versus frequency ratio F. (a) $<C_D>$, (b) C_{Lrms} . × - Results by [8] using feedback forcing; ○ - Present work (n_x, n_y = 361, 217; L_x, L_y = $20D$, $12D$); ◊ - Present work (n_x, n_y = 361, 325; L_x, L_y = $20D$, $18D$); △ - Numerical simulation by [9].

The results in the figure 1 shown that the shape curves of the coefficients is quite similar. All simulations presented a pick for $<C_D>$ when F is close to one and an increasing C_{Lrms} characterizing the lock-in phenomenon. Despite the use of low grid resolution, this study presented results for C_{Lrms} very close to the reference [9]. It could be observed a difference in the $<C_D>$ of approximately 0.2 between our results and those obtained in [9]. Numerical simulations by [10], found similar discrepancies for this hydrodynamic coefficient. They attribute these discrepancies to the $<C_D>$ obtained for simulations with the fixed cylinder. Simulation for the fixed cylinder were accomplished and its results for $<C_D>$, C_{Lrms} and f_s are compared in table 1. The results for $<C_D>$ shown that the discrepancy between the present work and [9] for fixed cylinder is approximately 0.2. This value is near to the differences observed in the drag curves for the oscillating cylinder (Figure 1). Numerical and experimental simulations for fixed cylinder at low Reynolds number are compared in [11]. Such authors presented a $<C_D> \approx 1.4$, at $Re \approx 190$, which is close to our results.

Comparing simulations with different computational domain, it was observed that as the vertical domain length L_y increases, the drag and lift coefficients decreases. These results indicate the existence of the blockage effect as expected.

Table 1. Comparative of the hydrodynamic coefficients $<C_D>$, C_{Lrms} and the Strouhal Number f_s for fixed cylinder.

Simulations	$<C_D>$	C_{Lrms}	f_s
IBM using feedback forcing by [8]	1.420	0.492	0.192
Present work (n_x, n_y: 361, 217; L_x, L_y: $20D$, $12D$)	1.488	0.516	0.199
Present work (n_x, n_y: 361, 325; L_x, L_y: $20D$, $18D$)	1.469	0.507	0.196
Results by [9]	1.287	0.443	0.195
Results by [11] at $Re \approx 190$	1.4	-	-

3.2. Vortex wakes

Instantaneous vorticity fields of the oscillating cylinder for $F = 0.8$ are shown in figure 2. Regarding the street wakes, significant alterations were not observed. The vortex shedding mode 2S was identified here for all simulations, corresponding to the shedding of two counter-rotating simple vortex at each oscillation cycle.

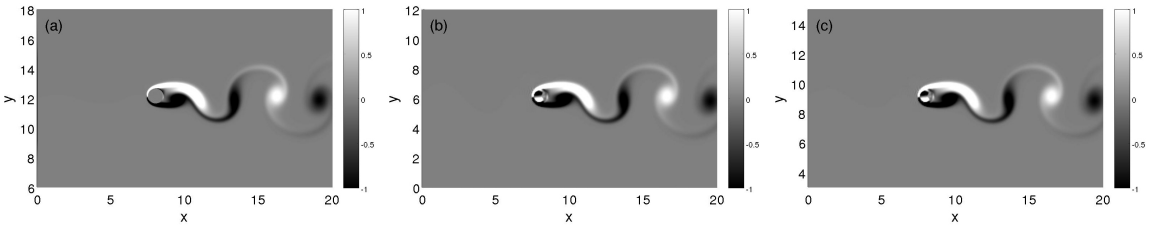

Figure 2. Instantaneous vorticity fields for simulations with $F = 0.8$: (a) IBM using feedback forcing by [8], (b) Present work (n_x, n_y: 361, 217; L_x, $L_y = 20D$, $12D$), (c) Present work (n_x, $n_y = 361$, 325; L_x, $L_y = 20D$, $18D$).

The figure 3 presents a comparative of the region next to the cylinder. In present simulations degraded results were expected due the lower grid resolution. However, the vicinity region of the cylinder presents quite similar results as shown by the isocontours of vorticity.

4. Conclusions

The results obtained shown that IBM technique used in the present work can represent the surface of a forced oscillating cylinder. The lock-in phenomenon was represented and the hydrodynamic coefficients are in agreement to other works in the current literature. Despite the use of lower grid resolution, this study presents results for the drag and lift forces very close to the others references (see, for instance [9] and [11]), and the vorticity fields are in agreement to others simulation of higher grid resolution.

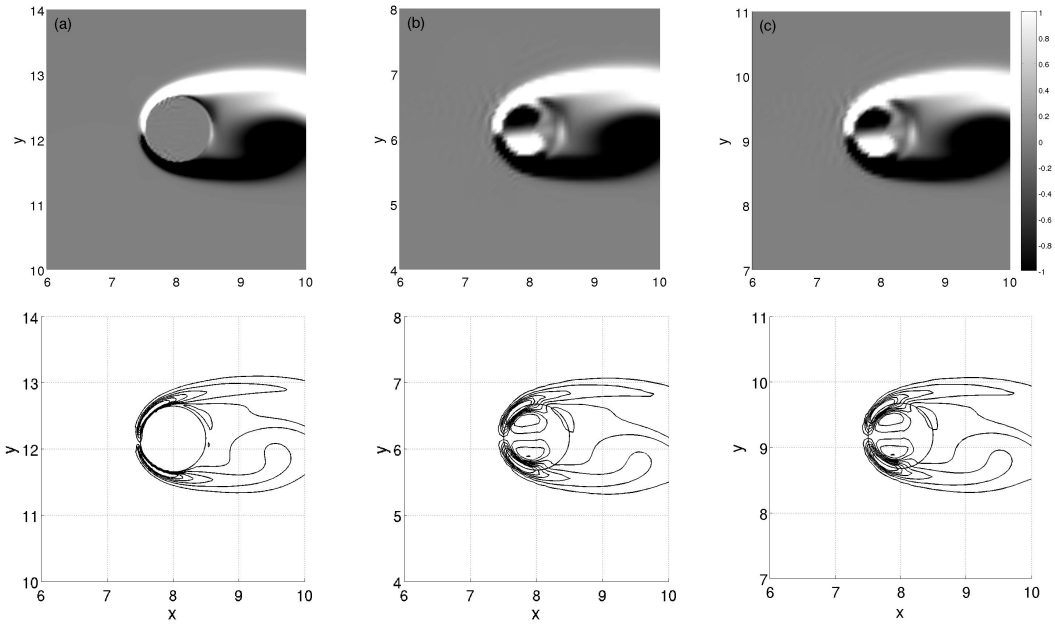

Figure 3. Instantaneous fields and isocontours (isolevels from -6 to 6 at each 1) of vorticity for simulations with $F = 0.8$: (a) IBM using feedback forcing by [8]; (b) Present work (n_x, n_y: 361, 217, L_x, $L_y = 20D$, $12D$); (c) Present work (n_x, $n_y =$ 361, 325, L_x, $L_y = 20D$, $18D$).

References

[1] Williamson C H K and Rohsko A 1988 *J. Fluid. Struct.* **2** 355
[2] Bishop R E D and Hassan A Y 1964 *Proc. R. Society* **277** 51
[3] Hoby S 2005 Master's thesis Université de Poitiers
[4] Parnaudeau P, Carlier J, Heitz D and Lamballais E 2008 *Phys. Fluids* **20** 085101
[5] Parnaudeau P, Lamballais E, Heitz D and Silvesrini J H 2003 *Proc. DLES-5* (Munich)
[6] Laizet S and Lamballais E 2009 *J. Comput. Phys.* **228** 5989
[7] Laizet S, Lamballais E and Vassilicos J C 2010 *Comput. Fluids* **39** 471
[8] Pinto L C, Schettini E B C and Silvestrini J H 2010 *Proc. BBVIV-6* (Italy) p 369
[9] Guilmineau E and Queutey P 2002 *J. Fluid. Struct.* **16** 773
[10] Placzek A, Sigrist J F and Hamdouni A 2009 *Comput. Fluids* **38** 80
[11] Sheard G J, Hourigan K and Thompson M C 2005 *J. Fluid Mech.* **526** 257